

Chapter 10 | Near-neutral Boundary Layers

10.1 Velocity-profile Laws

Strictly neutral stability conditions are rarely encountered in the atmosphere. However, during overcast skies and strong surface geostrophic winds, the atmospheric boundary layer may be considered near-neutral, and simpler theoretical and semiempirical approaches developed for neutral boundary layers by fluid dynamists and engineers can be used in micrometeorology. One must recognize, however, that, unlike in unidirectional flat-plate boundary layer and channel flows, the wind direction in the PBL changes with height in response to the Coriolis force due to the earth's rotation. Therefore, the wind distribution in the PBL is expressed in terms of either wind speed and direction, or the two horizontal components of velocity (see Figures 6.5–6.8).

10.1.1 The power-law profile

Measured velocity distributions in flat-plate boundary layer and channel flows can be represented approximately by a power-law expression

$$U/U_h = (z/h)^m \quad (10.1)$$

which was originally suggested by L. Prandtl with an exponent $m = 1/7$ for smooth surfaces. Here, h is the boundary layer thickness or half-channel depth. Since, wind speed does not increase monotonically with height up to the top of the PBL, a slightly modified version of Equation (10.1) is used in micrometeorology:

$$U/U_r = (z/z_r)^m \quad (10.2)$$

where U_r is the wind speed at a reference height z_r , which is smaller than or equal to the height of wind speed maximum; a standard reference height of 10 m is commonly used.

The power-law profile does not have a sound theoretical basis, but frequently it provides a reasonable fit to the observed velocity profiles in the lower part of the PBL, as shown in Figure 10.1. The exponent m is found to depend on both the surface roughness and stability. Under near-neutral conditions, values of m range from 0.10 for smooth water, snow and ice surfaces to about 0.40 for well-developed urban areas. Figure 10.2 shows the dependence of m on the roughness length or parameter z_0 , which will be defined later. The exponent m also increases with increasing stability and approaches one (corresponding to a linear profile) under very stable conditions. The value of the exponent may also depend, to some extent, on the height range over which the power law is fitted to the observed profile.

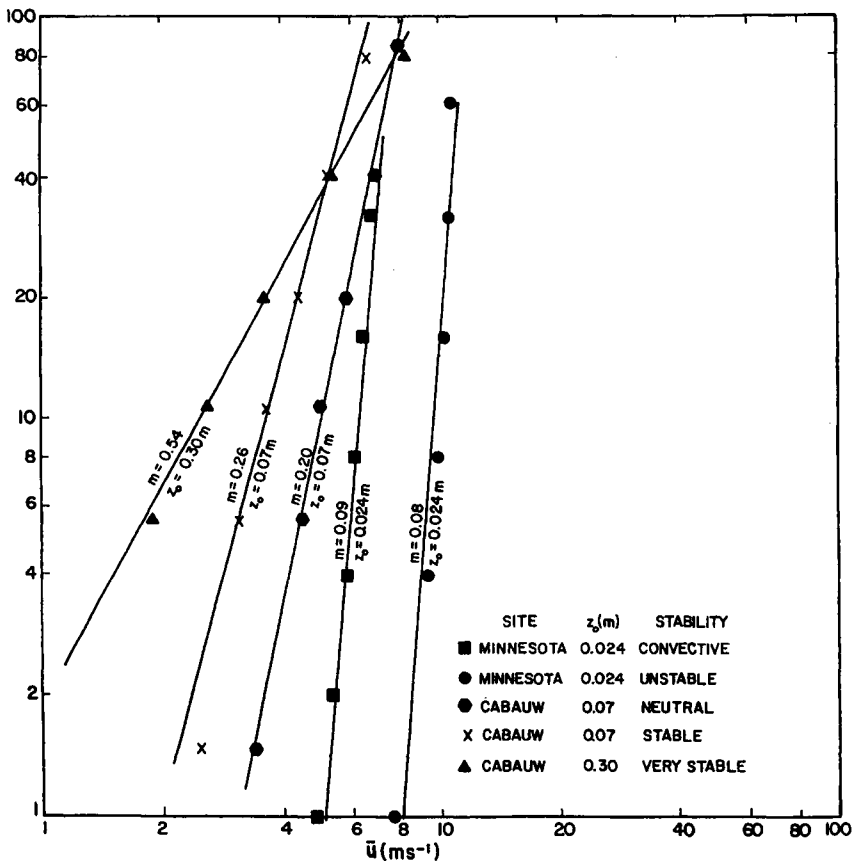


Figure 10.1 Comparison of observed wind speed profiles at different sites (z_0 is a measure of the surface roughness) under different stability conditions with the power-law profile. [Data from Izumi and Caughey (1976).]

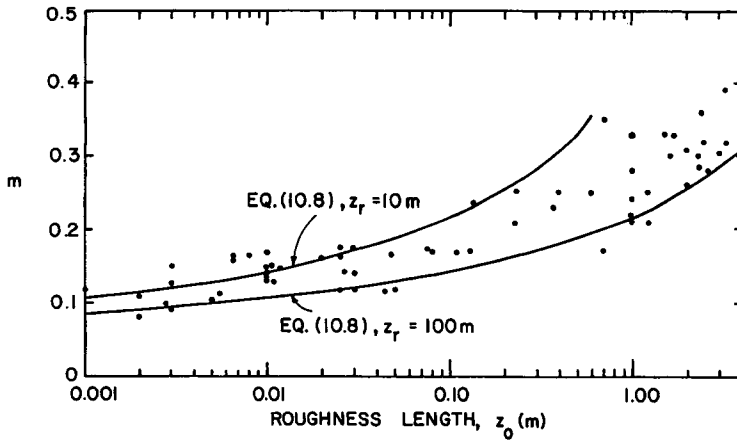


Figure 10.2 Variations of the power-law exponent with the roughness length for near-neutral conditions. [Data from Counihan (1975). Reprinted with permission from *Atmospheric Environment*. Copyright © (1975), Pergamon Journals Ltd.]

Note that the power-law wind profile would be appropriate only for the lower part of the PBL in which wind speed increases monotonically with height. At higher levels, wind speed may be specified differently (e.g., constant or linearly varying with height), depending on stability and other conditions (Arya, 1999, Chapter 4).

The power-law velocity profile implies a power-law eddy viscosity (K_m) distribution in the lower part of the boundary layer, in which the momentum flux may be assumed to remain nearly constant with height, i.e., in the constant stress layer. It is easy to show that

$$K_m/K_{mr} = (z/z_r)^n \quad (10.3)$$

with the exponent $n = 1 - m$, is consistent with Equation (10.2) in the surface layer. Equations (10.2) and (10.3) are called conjugate power laws and have been used extensively in theoretical formulations of atmospheric diffusion, including transfers of heat and water vapor from extensive uniform surfaces (Sutton, 1953). In such formulations eddy diffusivities of heat and mass are assumed to be equal or proportional to eddy viscosity, and thermodynamic energy and diffusion equations are solved for prescribed velocity and eddy diffusivity profiles in the above manner. When Equations (10.2) and (10.3) are used above the constant stress layer, however, the conjugate relationship $n = 1 - m$ need not be satisfied; this relationship may be too restrictive even in the surface layer.

10.1.2 The logarithmic profile law

Let us focus our attention now to the neutral surface layer over a flat and uniform surface in which Coriolis force can be ignored and the momentum flux may be considered constant, independent of height. Furthermore, we also exclude from our consideration any viscous sublayer that may exist over a smooth surface, or the canopy or roughness sublayer in which the flow is very likely to be disturbed by individual roughness elements. For the remaining fully turbulent, horizontally homogeneous surface layer, a simple similarity hypothesis can be used to obtain the velocity distribution, namely, the mean wind shear $\partial U/\partial z$ is dependent only on the height z above the surface (more appropriately, above a suitable reference plane near the surface), the surface drag, and the fluid density, i.e.,

$$\partial U/\partial z = f(z, \tau_0, \rho) = f(z, \tau_0/\rho) \quad (10.4)$$

An implied assumption in this similarity hypothesis is that the influence of other possible parameters, such as the surface roughness, horizontal pressure gradients (geostrophic winds), and the PBL height, is fully accounted for in τ_0 , which then determines the velocity gradients in the surface layer. Note that it is appropriate to combine τ_0 and ρ into their ratio τ_0/ρ , which represents the kinematic momentum flux, because the dependent variable does not contain any mass dimension.

The only characteristic velocity scale given by the above surface layer similarity hypothesis is the so-called friction velocity $u_* \equiv (\tau_0/\rho)^{1/2}$, and the only characteristic length scale is z . Then, from dimensional analysis it follows that the dimensionless wind shear

$$(z/u_*)(\partial U/\partial z) = \text{const.} = 1/k \quad (10.5)$$

where k is called von Karman's constant.

The above similarity relation has been verified by many observed velocity profiles in laboratory boundary layer, channel, and pipe flows, as well as in the near-neutral atmospheric surface layer. The von Karman constant is presumably a universal constant for all surface or wall layers. However, it is an empirical constant with a value of about 0.40; it has not been possible to determine it with an accuracy better than 5% (Hogstrom, 1985).

Note that Equation (10.5) also follows from the mixing length and eddy viscosity hypotheses, if one assumes that $l = kz$ and/or $K_m = kzu_*$ in the constant-flux surface layer. Integration of Equation (10.5) with respect to z gives the well-known logarithmic velocity profile law,

$$U/u_* = (1/k) \ln(z/z_0) \quad (10.6)$$

in which z_0 has been introduced as a dimensional constant of integration and is commonly referred to as the roughness parameter or roughness length. The physical significance of z_0 and its relationship to surface roughness characteristics will be discussed later.

For a comparison of the power-law and logarithmic wind profiles, Equation (10.6) can be written as

$$U/U_r = 1 + \ln(z/z_r)/\ln(z_r/z_0) \quad (10.7)$$

Figure 10.3 compares the plots of U/U_r versus z/z_r , according to Equations (10.2) and (10.7), for different values of m and z_r/z_0 , respectively. There is no exact correspondence between these two profile parameters, because the two profile shapes are different. An approximate relationship can be obtained by matching the velocity gradients, in addition to the mean velocities, at the reference height z_r :

$$m = \frac{d(\ln U)}{d(\ln z)} = \frac{z}{U} \frac{\partial U}{\partial z} \bigg|_{z=z_r} = \left(\frac{z_r}{z_0} \right)^{-1} \quad (10.8)$$

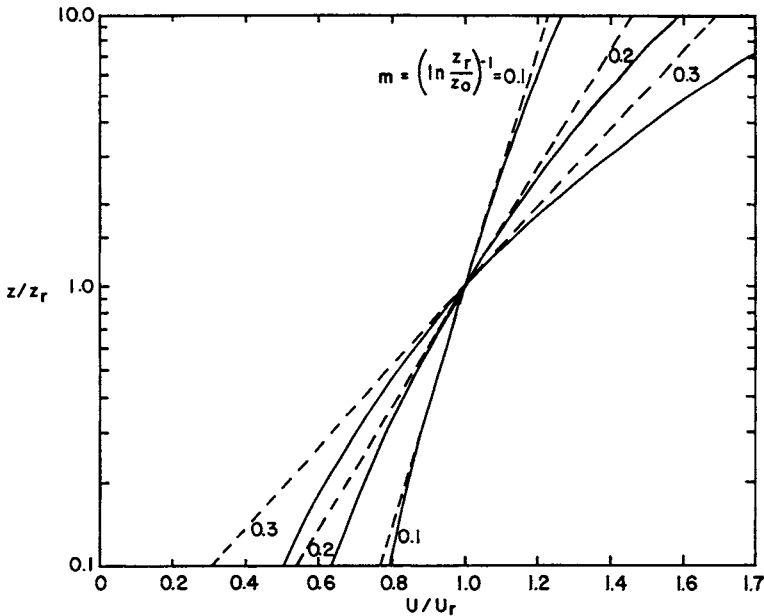


Figure 10.3 Comparison of hypothetical wind profiles following the power-law Equation (10.2) (—) and the log-law Equation (10.7) (---) with their parameters related by Equation (10.8).

Even with this type of matching, the two profiles deviate more and more as z deviates farther and farther from the matching height z_r . The theoretical relationship given by Equation (10.8) between the power-law exponent m and the surface roughness parameter is also compared with observations in Figure 10.2. For different data sets represented in that figure, z_r lies in the range between 10 and 100 m.

The logarithmic profile law has a sounder theoretical and physical basis than the power-law profile, especially within the neutral surface layer. The former implies linear variations of eddy viscosity and mixing length with height, irrespective of the surface roughness, while the power-law profile implies the incorrect and unphysical, nonlinear behavior of K_m and l_m , even close to the surface.

Many observed wind profiles near the surface under near-neutral conditions have confirmed the validity of Equation (10.6) up to heights of 20–200 m, depending on the PBL height. Figure 10.4 illustrates some of the observed wind

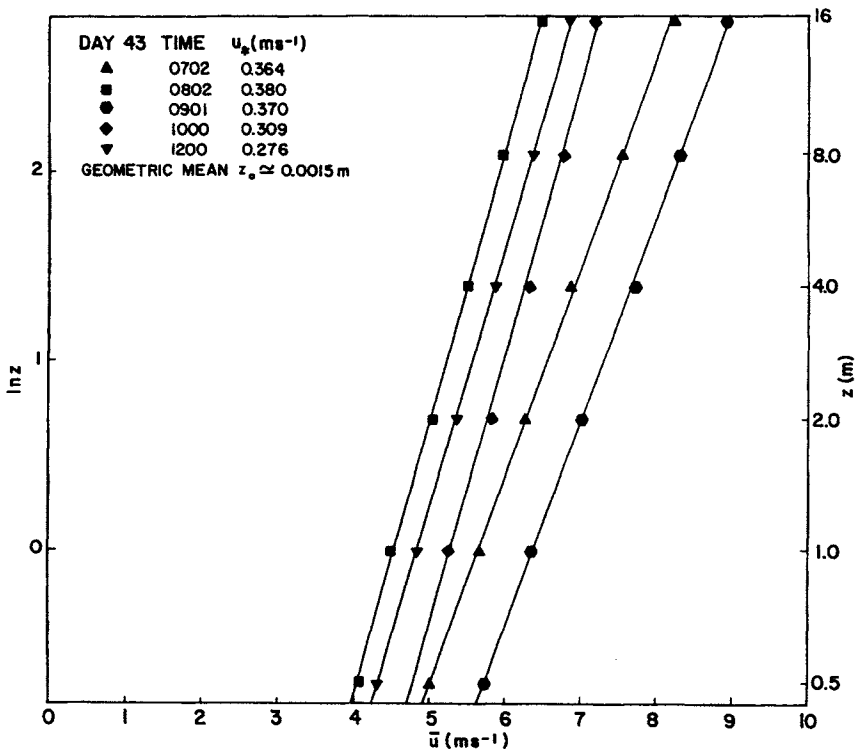


Figure 10.4 Comparison of the observed wind profiles in the neutral surface layer of Wangara Day 43 with the log law [Equation (10.6)] (solid lines). [Data from Clarke *et al.* (1971).]

profiles during the Wangara Experiment which was conducted over a low grass surface in southern Australia. These plots of $\ln z$ versus U also illustrate how the best-fitted straight line through observed data points can be used to estimate the surface-layer parameters u_* and z_0 . Note that, according to Equation (10.6), the slope of the line must be equal to k/u_* , while its intercept on the $\ln z$ axis where $U = 0$ must be equal to $\ln z_0$. Thus estimates of slope and intercept of the best-fitted line yield u_* and z_0 . If there are several wind profiles available at the same site, one can determine z_0 as the geometric mean of the values obtained from individual profiles.

In the engineering fluid mechanics literature, Equation (10.6) is referred to as the law of the wall, which has been found to hold in all kinds of pipe and channel flows, as well as in boundary layers. There, the distinction is made between aerodynamically smooth and rough surfaces. A surface is considered aerodynamically smooth if the small-scale surface protuberances or irregularities are sufficiently small to allow the formation of a laminar or viscous sublayer in which surface protuberances are completely submerged. If small-scale surface irregularities are large enough to prevent the formation of a viscous sublayer, the surface is considered aerodynamically rough. It is found from laboratory measurements that the thickness of the laminar sublayer in which the velocity profile is linear is about $5\nu/u_*$. For atmospheric flows the sublayer thickness would be of the order of 1 mm or less, while surface protuberances are generally larger than 1 mm. Therefore, almost all natural surfaces are aerodynamically rough; the only exceptions might be smooth ice, snow, and mud flats, as well as water surfaces under weak winds ($U_{10\text{ m}} < 3\text{ m s}^{-1}$). The law of the wall (velocity-profile law) for an aerodynamically smooth surface is usually expressed in the form (Monin and Yaglom, 1971, Chapter 3)

$$\frac{U}{u_*} = \frac{1}{k} \ln \frac{u_* z}{\nu} + 5.1 \cong \frac{1}{k} \ln \left(\frac{u_* z}{0.13\nu} \right) \quad (10.9)$$

in which the characteristic height scale of the viscous sublayer (ν/u_*) is used in place of z_0 for a rough surface, and the numerical constant is evaluated from laboratory measurements in smooth flat-plate boundary layer and channel flows.

A comparison of Equations (10.6) and (10.9) shows that, if the former is used to represent wind profiles over a smooth surface, one should expect the roughness parameter to decrease with increasing u_* , according to the relation $z_0 \cong 0.13\nu/u_*$. For a rigid, aerodynamically rough surface, however, z_0 is expected to remain constant, independent of u_* . Some surfaces are neither smooth nor completely rough, but fall into a transitional roughness regime. In nature, lake, sea and ocean surfaces may fall into this transition between

smooth and rough surfaces at moderate wind speeds ($2.5 < U_{10} < 7.5 \text{ m s}^{-1}$) (Kitaigorodski, 1970).

The transfer of momentum from the atmosphere to the ocean or sea surface is of considerable importance to meteorologists, as well as to physical oceanographers. A part of this momentum goes into the generation of surface waves, while the remaining portion is responsible for setting up drift currents and turbulence in the upper layers of the ocean. The relative partitioning of momentum between these different modes of motion in water depends on such factors as the stage of wave growth, duration and fetch of winds, etc., and is not easy to determine. But the total momentum exchange can be determined from measurements in the atmospheric surface layer, well above the level of highest wave crests.

When one considers extending the 'law of the wall' similarity to air flow over a moving water surface, the effects of both the surface drift currents and surface waves should be taken into account. The surface current, which is typically 3–5% of the wind speed at 10 m, but can be much stronger in certain regions (e.g., the Gulf Stream, Kuroshio, and other ocean currents), can easily be taken into account by considering the air motion relative to that of surface water ($U = U_a - U_w$). The influence of moving surface waves on mean wind profile in the surface layer is much more difficult to discern.

10.1.3 The velocity-defect law

Above the surface layer, the Coriolis effects become significant and it is more appropriate to consider the deviations of actual velocity from the geostrophic velocity. For flat-plate boundary layer and channel flows, similarity considerations for the deviations of velocity from the ambient velocity lead to the so-called velocity-defect law (Monin and Yaglom, 1971, Chapter 3)

$$(U - U_\infty)/u_* = F(z/h) \quad (10.10)$$

The analogous geostrophic departure laws proposed for the neutral barotropic PBL are (Tennekes, 1982):

$$\begin{aligned} (U - U_g)/u_* &= F_u(fz/u_*) \\ (V - V_g)/u_* &= F_v(fz/u_*) \end{aligned} \quad (10.11)$$

These are based on the similarity hypothesis for the barotropic, neutral PBL that departures in mean velocity components from their geostrophic values are functions of z , u_* and f only. This similarity hypothesis was originally proposed

by Kazanski and Monin (1961). It also implies that the neutral PBL height must be proportional to u_*/f , i.e., $h = cu_*/|f|$ where c is an empirical constant with estimated values between 0.2 and 0.3.

A satisfactory confirmation of Equation (10.11) and empirical determination of the similarity functions F_u and F_v has been made from atmospheric observations under near-neutral stability conditions. A strictly neutral, stationary, and barotropic PBL, which is not constrained by any inversion from above, is so rare in the atmosphere that relevant observations of the same do not exist. The averages of wind profiles measured under slightly unstable and slightly stable conditions appear to follow the above similarity scaling (Clarke, 1970; Nicholls, 1985). Some laboratory simulations of the neutral Ekman layer in a rotating wind tunnel flow have also confirmed the same. Of course, there is plenty of experimental support for the validity of the velocity-defect law [Equation (10.10)] in nonrotating flows.

Example Problem 1

The following mean wind speeds were measured over a short grass surface under near-neutral stability conditions:

z (m):	0.5	1	2	4	8	16
U (m s ⁻¹):	7.82	8.66	9.54	10.33	11.22	12.01

- Determine the roughness length and friction velocity from a plot of $\ln z$ versus U .
- Using appropriate similarity relations, estimate eddy viscosity and mixing length at 10 and 100 m.

Solution

- Plotting $\ln z$ versus U and drawing the best-fitted regression line through the data points, or simply regressing $\ln z$ against U in a programmable calculator, one obtains

$$\ln z = 0.824U - 7.15$$

Comparing this with Equation (10.6), which can be rewritten as

$$\ln z = \frac{k}{u_*} U - \ln z_0$$

we obtain $k/u_* = \text{slope of the line} = 0.824 \text{ s m}^{-1}$, or

$$u_* = 0.40/0.824 = 0.485 \text{ m s}^{-1},$$

and $\ln z_0 = -7.15$, so that

$$z_0 \cong 7.9 \times 10^{-4} \text{ m} = 0.079 \text{ mm.}$$

(b) In the neutral surface layer, eddy viscosity and mixing length are given by

$$K_m = kzu_*; l_m = kz$$

from which the following values can be estimated at the desired height levels (10 and 100 m):

z (m)	K_m ($\text{m}^2 \text{s}^{-1}$)	l_m (m)
10	1.94	4.0
100	19.40	40

10.2 Surface Roughness Parameters

The aerodynamic roughness of a flat and uniform surface may be characterized by the average height (h_0) of the various roughness elements, their areal density, characteristic shapes, and dynamic response characteristics (e.g., flexibility and mobility). All the above characteristics would be important if one were interested in the complex flow field within the roughness or canopy layer. There is not much hope for a generalized and, at the same time, simple theoretical description of such a three-dimensional flow field in which turbulence dominates over the mean motion. In theoretical and experimental investigations of the fully developed surface layer, however, the surface roughness is characterized by only one or two roughness characteristics which can be empirically determined from wind-profile observations.

10.2.1 Roughness length

The roughness length parameter z_0 introduced in Equation (10.6) is one such characteristic. In practice, z_0 is determined from the least-square fitting of Equation (10.6) through the wind-profile data, or by graphically plotting $\ln z$ versus U and extrapolating the best-fitted straight line down to the level where $U = 0$; its intercept on the ordinate axis must be $\ln z_0$. One should note, however, that this is only a mathematical or graphical procedure for estimating z_0 and that Equation (10.6) is not expected to describe the actual wind profile

below the tops of roughness elements. An assumption implied in the derivation of (10.6) is that $z_0 \ll z$.

Empirical estimates of the roughness parameter for various natural surfaces can be ordered according to the type of terrain (Figure 10.5) or the average height of the roughness elements (Figure 10.6). Although z_0 varies over five orders of magnitude (from 10^{-5} m for very smooth water surfaces to several meters for forests and urban areas), the ratio z_0/h_0 falls within a much narrower range (0.03–0.25) and increases gradually with increasing height of roughness elements. For uniform sand surfaces Prandtl and others have suggested a value of $z_0/h_0 \cong 1/30$. An average value of $z_0/h_0 = 0.15$ has been determined for various crops and grasslands; the same may also be used for many other natural surfaces (Plate, 1971). Figure 10.5 gives some typical values of z_0 for different types of surfaces and terrains. Figure 10.6 relates z_0 to h_0 for different types of crop canopies.

Wind-profile measurements from fixed towers in shallow coastal waters and from stable floating buoys (ships are not suitable for this, as they present too much of an obstruction to the air flow) over open oceans also follow the logarithmic law [Equation (10.6)] under neutral stability conditions. However, the roughness parameter (z_0) determined from this is found to be related to both the wind and wave fields in a rather complex manner and can vary over a very wide range (say, 10^{-5} – 10^{-2} m).

There have been a number of semiempirical and theoretical attempts at relating z_0 to the friction velocity, as well as to the average height, the phase speed, and the stage of development of surface waves. The simplest and still the most widely used relationship is that proposed by Charnock (1955) on the basis of dimensional arguments

$$z_0 = a(u_*^2/g) \quad (10.12)$$

where a is an empirical constant. The basic assumptions implied in Charnock's hypothesis (z_0 is uniquely determined by u_* and g) are that the winds are blowing steadily and long enough for the wave field to be in complete equilibrium with the wind field, independent of fetch, and that the surface is aerodynamically rough.

Individual estimates of z_0 plotted as a function of u_*^2/g invariably show large scatter, because they usually pertain to different fetches and different stages of wave development and also because of large errors in the experimental determination of z_0 . However, when the available data sets are block averaged, a definite trend of z_0 increasing in proportion to u_*^2/g does emerge. Figure 10.7 shows such block-averaged data compiled from some 33 experimental sets of wind profile and drag data (Wu, 1980). Note that Charnock's relation is verified, particularly for large values of z_0 and u_*^2/g , and $a \cong 0.018$. Empirical

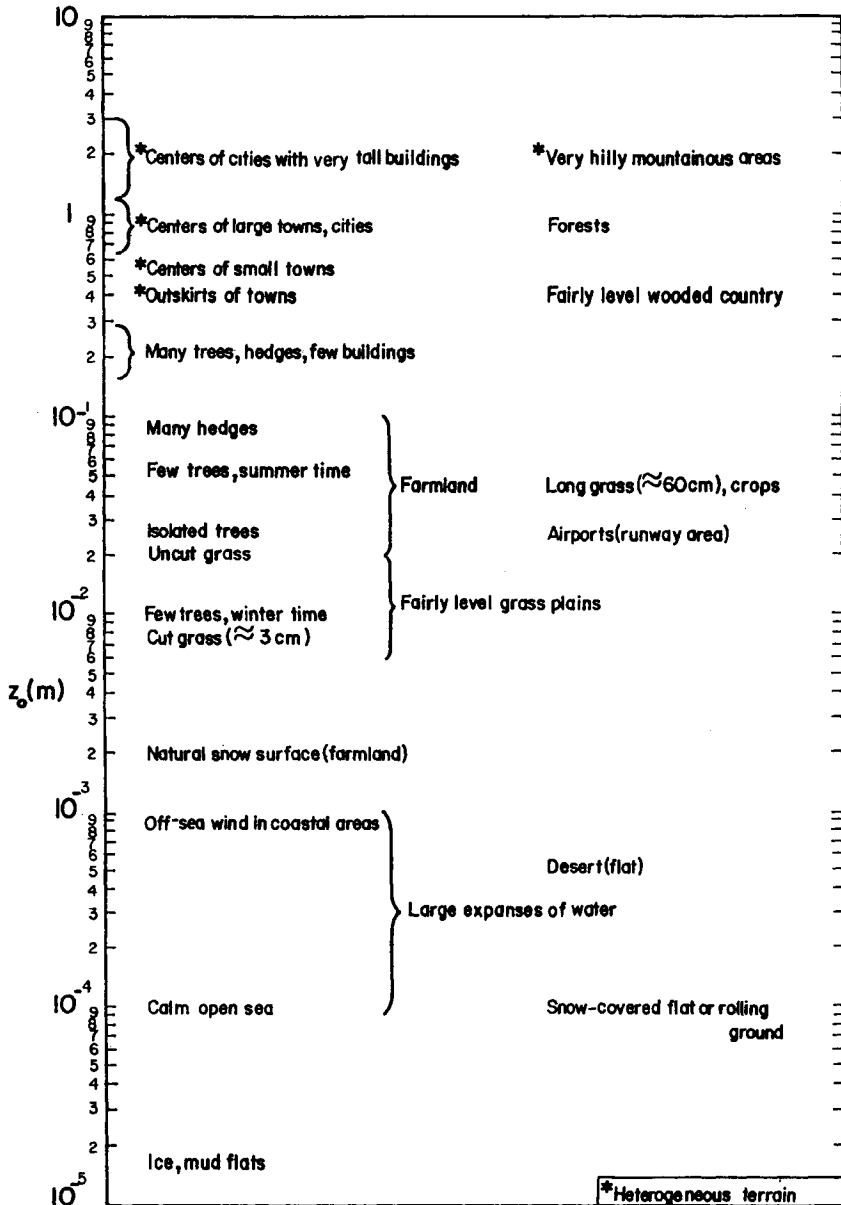


Figure 10.5 Typical values, or range of values, of the surface roughness parameter for different types of terrain. [From tables by the Royal Aeronautical Society (1972).]

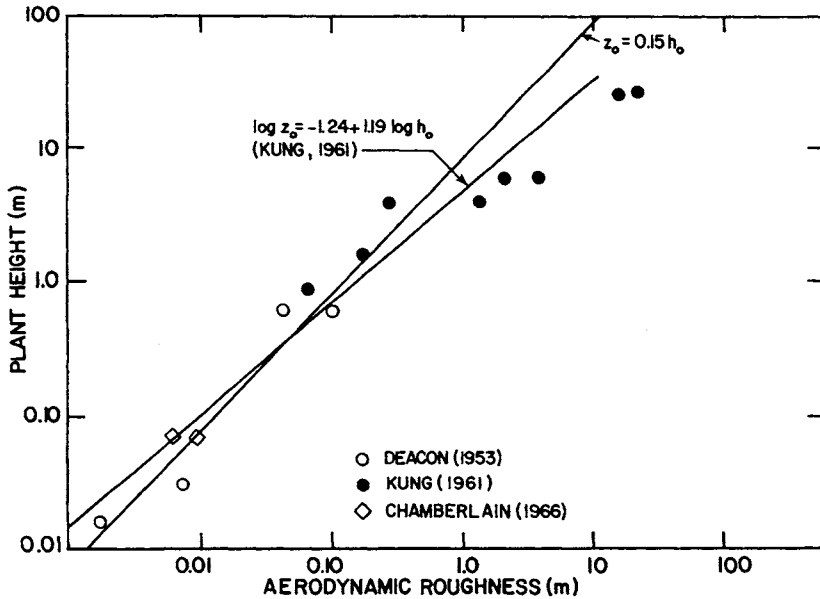


Figure 10.6 Relationship between the aerodynamic roughness parameter and the average vegetation height. [From Plate (1971).]

estimates of a by other investigators have ranged between 0.01 and 0.035 (Garratt, 1992).

The simple state of affairs assumed in Charnock's hypothesis rarely exists over lakes and oceans. More frequently, the wave field is not in equilibrium with local winds, but depends on the strength, fetch, and time history of the wind field. At low wind speeds, the surface can also become aerodynamically smooth, or be in a transitional regime between smooth and rough. A comprehensive treatment of sea-surface roughness at different development stages of wind-generated waves is given by Kitaigorodski (1970). The fundamental parameter indicating the stage of wave development, in his theory, is the ratio C_0/u_* , where C_0 is the phase speed of the most dominant (corresponding to the peak in the wave-height spectrum) waves. It is shown that only in the equilibrium stage of wave development is z_0 proportional to u_*^2/g . Furthermore, on the basis of analogy with the aerodynamic roughness of a rigid surface, z_0 is assumed proportional to h_0 for a completely rough surface; proportional to v/u_* for an aerodynamically smooth surface; and a function of both h_0 and v/u_* in the transitionally smooth or rough regime. Kitaigorodski has suggested plausible expressions for the roughness parameter for the various combinations of roughness and wave regimes, some of them involving still unknown empirical

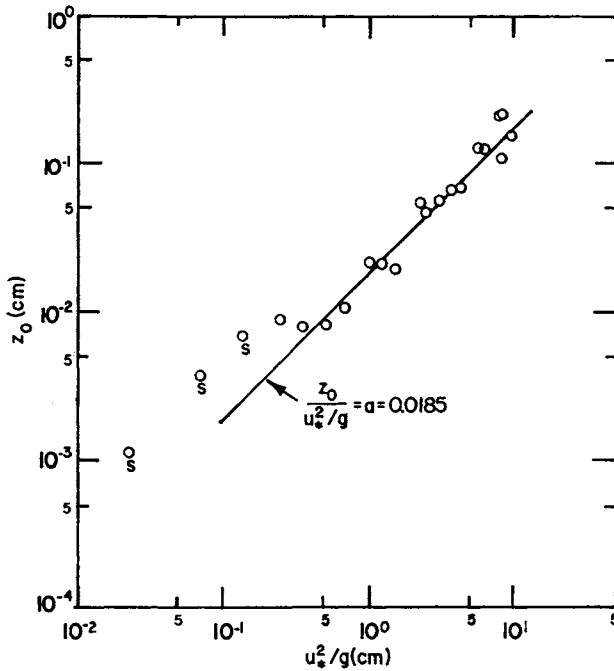


Figure 10.7 Observed roughness parameter of sea surface as a function of u_*^2/g compared with Charnock's (1955) formula. [After Wu (1980).]

constants or functions. For the fully-developed wave field, a simple interpolation relation

$$z_0 = a \frac{u_*^2}{g} + 0.13 \frac{v}{u_*} \quad (10.13)$$

has been suggested (Smith *et al.*, 1996).

At low wind speeds (say $U_{10} < 7 \text{ m s}^{-1}$) and in the early stages of wave development, the sea surface appears to be remarkably smooth, before waves start to break. In fact, the aerodynamic roughness of even a fully developed sea under a tropical storm is observed to be less than that of mown grass. This is largely due to the fact that waves are generated by and move along with the wind and do not offer as much resistance to the flow as would an immobile surface with similar shape. There is also strong evidence suggesting that sea-surface drag is primarily due to small ripples and wavelets with phase speeds less than the near-surface wind speed, and that large waves make only a minor contribution to the drag.

Different surface roughness regimes mentioned earlier are found to occur over oceans. In the absence of swell, the sea surface is found to be aerodynamically smooth during calm and weak winds ($U_{10} < 2.5 \text{ m s}^{-1}$), transitionally rough in moderate winds ($2.5 \leq U_{10} \leq 7.5 \text{ m s}^{-1}$), and completely rough in strong winds ($U_{10} > 7.5 \text{ m s}^{-1}$). The above criteria should be considered only approximate and limited to fully developed (equilibrium) wind-generated waves. The data points corresponding to small values of u_*^2/g in Figure 10.7 probably belong to the transitional roughness regime.

10.2.2 Displacement height

For very rough and undulating surfaces, the soil–air or water–air interface may not be the most appropriate reference datum for measuring heights in the surface layer. The air flow above the tops of roughness elements is dynamically influenced by the ground surface as well as by individual roughness elements. Therefore, it may be argued that the appropriate reference datum should lie somewhere between the actual ground level and the tops of roughness elements. In practice, the reference datum is determined empirically from wind-profile measurements in the surface layer under near-neutral stability conditions. The modified logarithmic wind-profile law used for this purpose is

$$U/u_* = (1/k) \ln[(z' - d_0)/z_0] \quad (10.14)$$

in which d_0 is called the zero-plane displacement or displacement height and z' is the height measured above the ground level.

For a plane surface, d_0 is expected to lie between zero and h_0 , depending on the areal density of roughness elements. The displacement height may be expected to increase with increasing roughness density and approach a value close to h_0 for very dense canopies in which the flow within the canopy might become stagnant, or independent of the air flow above the canopy. These expectations are indeed borne out by empirical estimates of d_0 for vegetative canopies (see Figure 10.8) which indicate that the appropriate datum for wind-profile measurements over most vegetative canopies is displaced above the ground level by 70–80% of the average height of vegetation. The zero-plane displacement in an urban boundary layer can similarly be expected to be a large fraction of the average building height.

After the mean height of roughness elements, the next important characteristic of roughness morphology is the ratio $\lambda = A_f/A_h$, where A_f is the total frontal area of roughness elements and A_h is the horizontal area covered by them. As the frontal area density (λ) increases, the ratio d_0/h_0 may be expected to increase monotonically to its maximum value of one. The ratio z_0/h_0 is also

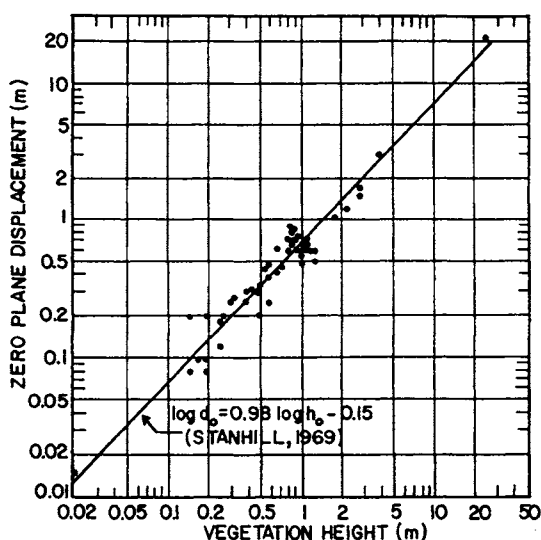


Figure 10.8 Relationship between the zero-plane displacement and average vegetation height for different types of vegetation. [After Stanhill (1969).]

expected to increase and attain its maximum value at some optimum value of $\lambda < 1$. Wind tunnel experiments with regular arrays of simulated roughness elements have confirmed these expectations (McDonald *et al.*, 1998). Methods of determining surface roughness parameters from an analysis of surface morphometry of urban areas have also been suggested (Grimmond and Oke, 1999).

Figure 10.9 shows a verification of Equation (10.14) against observed wind profiles over bare and vegetative surfaces, using appropriate estimates of z_0 and d_0 for each surface.

10.3 Surface Drag and Resistance Laws

A direct measurement of the wind drag or stress on a relatively smooth surface can be made with an appropriate drag plate of a nominal diameter of 1–2 m and surface representative of the terrain around it (Bradley, 1968). The larger the surface roughness, the more difficult it becomes for the drag plate to represent (simulate) such a roughness. Therefore, this method of drag measurement is limited to flat and uniform surfaces which are bare or have low vegetation. In most other cases, and also when drag-plate measurements cannot be made, the surface stress is determined indirectly from wind measurements in the surface layer.

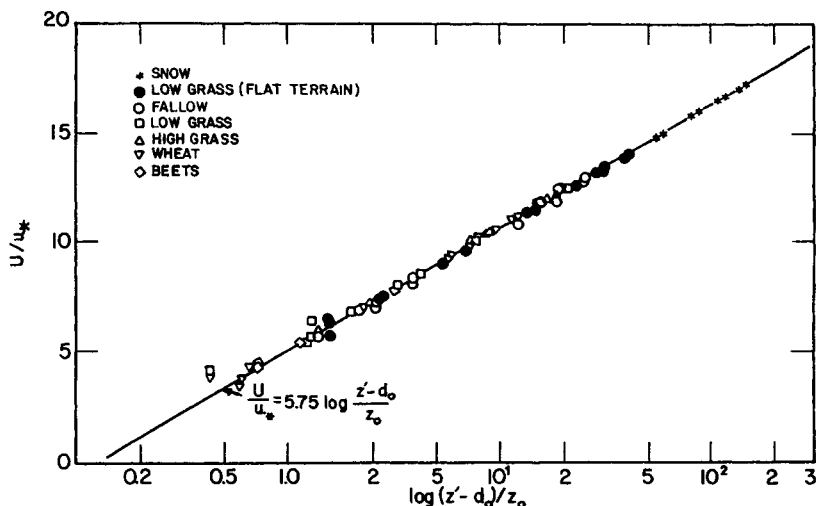


Figure 10.9 Comparison of observed velocity profiles over crops with the log law [Equation (10.14)]. [From Plate (1971).]

10.3.1 Surface drag law

If mean winds are observed at a standard reference height z_r , the surface stress can be determined using a drag relation

$$\tau_0 = \rho C_D U_r^2 \quad (10.15)$$

in which C_D is a dimensionless drag coefficient which depends on the surface roughness (more appropriately, on the ratio z_r/z_0) and atmospheric stability near the surface. In particular, for near-neutral stability, the drag coefficient is given by

$$C_{DN} = k^2 / [\ln(z_r/z_0)]^2 \quad (10.16)$$

which follows from Equations (10.6) and (10.15). Note that for a given z_r , C_{DN} increases with increasing surface roughness. For a standard reference height of 10 m, values of C_{DN} range from 1.0×10^{-3} for large lake and ocean surfaces at moderate wind speeds ($U_{10} < 6 \text{ m s}^{-1}$) to 7.5×10^{-3} for tall crops and moderately rough ($z_0 < 0.1 \text{ m}$) surfaces. For very rough surfaces (e.g., forests and urban areas), however, a reference height of 10 m would not be adequate; it must be at least 1.5 times the height of roughness elements.

There has been considerable interest in knowing the dependence of C_{DN} over ocean surfaces on wind speed, sea state, and other factors. To this end, many experimental determinations of C_{DN} have been made by different investigators, using different measurement techniques. Early determinations were largely based on rather crude estimates of the tilt of water surface and the geostrophic departure of flow in the PBL, and are not considered very reliable. Later, the sea-surface drag was determined by using the more reliable eddy correlation, gradient, and profile methods. A comprehensive review of the existing data on C_D up to 1975 was made by Garratt (1977). After applying the appropriate corrections for atmospheric stability and actual observation height, the neutral drag coefficient C_{DN} , referred to the standard height of 10 m, was obtained as a function of wind speed at 10 m (U_{10}).

Figure 10.10(a) shows the block-averaged values of $C_{DN} \pm 1$ standard deviation (indicated by vertical bars) for intervals of U_{10} of 1 m s^{-1} , based on the eddy correlation method (closed circles) and wind-profile method (open circles). The number of data points used for averaging in each 1 m s^{-1} interval are also indicated above the abscissa axis (the top line refers to closed circles and the bottom line to open circles). Note that there are too few data points to give reliable estimates of C_{DN} at high wind speeds ($U_{10} > 15 \text{ m s}^{-1}$). However, some investigators have inferred the surface drag in hurricanes, using the geostrophic departure method. Others have measured C_{DN} at high wind speeds in laboratory wind flume experiments. Figure 10.10(b) shows that there is a remarkable similarity between the hurricane data and wind flume data (usually referred to a height of 10 cm, assuming a scaling factor of 100:1), despite the large expected errors in the former and dissimilarity of wave fields in the two cases.

Considering the overall block-averaged data for the whole wide range of wind speeds represented in Figure 10.10, there is no doubt that C_{DN} increases with wind speed. The trend appears to be quite consistent with Charnock's formula [Equation (10.12)], which, in conjunction with Equations (10.15) and (10.16) yields

$$\ln C_{DN} + kC_{DN}^{-1/2} = \ln(gz/aU_r^2) \quad (10.17)$$

After determining the best-fitting value of $a \cong 0.0144$ with $k = 0.41$ (for the more commonly used value of $k = 0.4$, one would obtain $a \cong 0.017$, which is closer to the value indicated in Figure 10.7), from a regression of $\ln C_{DN} + kC_{DN}^{-1/2}$ on $\ln U_{10}$, Equation (10.17) is represented in Figures 10.10a and b. In the completely rough regime ($U_{10} > 7 \text{ m s}^{-1}$), in particular, Charnock's relation is in good agreement with the experimental data. The variation of C_{DN} with U_{10} can also be approximated by a simple linear relation (Garratt, 1977)

$$C_{DN} = (0.75 + 0.067U_{10}) \times 10^{-3} \quad (10.18)$$

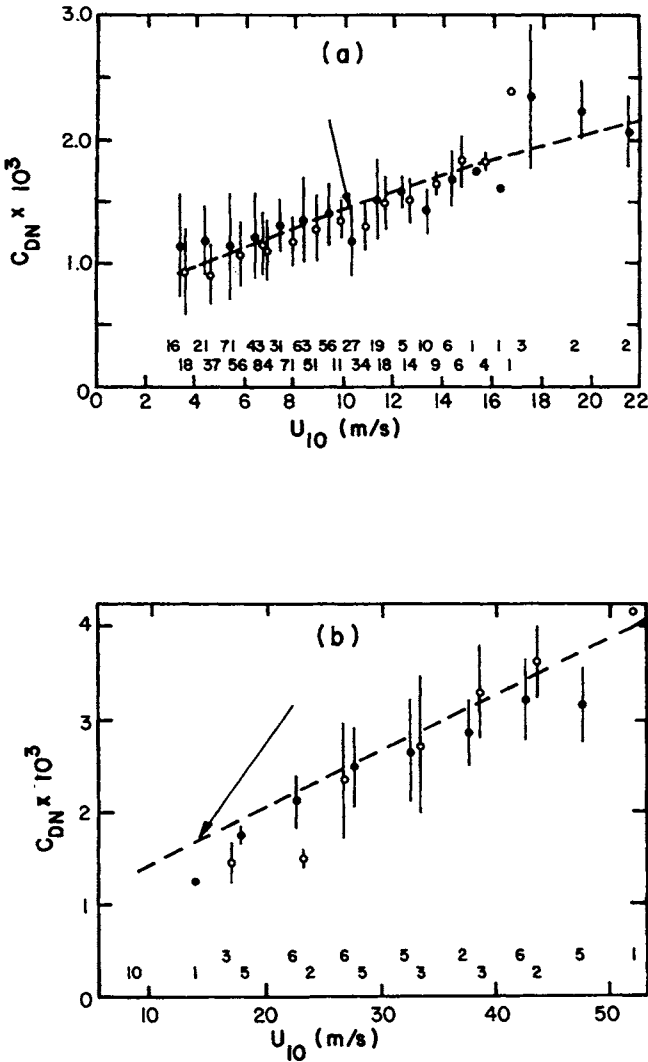


Figure 10.10 Neutral drag coefficient as a function of wind speed at 10 m height compared with Charnock's formula [Equation (10.17), indicated by arrows in (a) and (b)] with $a = 0.0144$. Block-averaged values are shown for (a) 1 m s^{-1} intervals, based on eddy correlation and profile methods, and (b) 5 m s^{-1} intervals, based on geostrophic departure method and wind flume simulation experiments. [After Garratt (1977).]

in which U_{10} is to be expressed in meters per second. A linear relationship, similar to Equation (10.18), is also suggested by other measurements of drag in gale-force winds (Smith, 1980).

There is some controversy over the variation of C_{DN} with U_{10} at low and moderate wind speeds (say, $U_{10} < 7.5 \text{ m s}^{-1}$). At very low wind speeds ($U_{10} < 2.5 \text{ m s}^{-1}$), observations from laboratory flume experiments and from over lakes and oceans indicate a slight tendency for C_{DN} to decrease with the increase in wind speed, as would be expected for an aerodynamic smooth surface. But sea surface is rarely completely smooth; ripples and wavelets generated by weak to moderate winds give it a moderate roughness, which is transitional between smooth and completely rough regimes. Some investigators have argued that the dependence of C_{DN} on U_{10} should be weak, if any, in this transitional regime ($2.5 < U_{10} < 7.5 \text{ m s}^{-1}$). The data of Figure 10.10 do suggest a weaker dependence of C_{DN} on U_{10} in this range. Other oceanic data have even indicated a nearly constant value of $C_{DN} \cong 1.2 \times 10^{-3}$ in the moderate range of wind speeds (Kraus, 1972).

Few investigators have sought to investigate the dependence of C_{DN} on wind direction, fetch, and sea-state parameters, such as C_0/u_* (Kitaigorodski, 1970; SethuRaman, 1978; Smith, 1980). There is only a slight tendency for the drag coefficient to decrease with increasing fetch. It has also been argued that the coefficient a in Charnock's formula should decrease with increasing C_0/u_* and may reach a constant asymptotic value only at the equilibrium stage of wave development. This would imply that C_{DN} should also decrease with increasing C_0/u_* . An observational evidence in support of such a trend is given by SethuRaman (1978), who also shows dramatic changes in C_{DN} in response to a rapid shift in wind direction.

10.3.2 Geostrophic drag relations

Alternative parameterizations of the surface drag use the surface geostrophic wind speed (G_0), or the actual wind speed at the top of the PBL, instead of the near-surface wind in expressing the surface stress, e.g.,

$$\tau_0 = \rho C_D G_0^2 \quad (10.19)$$

in which the value of C_D is expected to be smaller than that in Equation (10.15). The ratio $u_*/G_0 = C_D^{1/2}$ is often called the geostrophic drag coefficient and denoted by c_g . For the neutral PBL, c_g can be expressed as a function of the

surface Rossby number, G_0/fz_0 , using the so-called geostrophic resistance laws (Tennekes, 1982):

$$\begin{aligned} U_g/u_* &= \frac{1}{k} [\ln(u_*/fz_0) - A] \\ V_g/u_* &= -B/k \end{aligned} \quad (10.20)$$

where A and B are similarity constants.

An elegant derivation of the above resistance laws from the asymptotic matching of the neutral surface layer and the PBL similarity wind-profile relations (10.6) and (10.11) is given by Tennekes (1982). The similarity constants have been empirically determined from the observed wind profile and geostrophic winds under near-neutral conditions. Earlier estimates from observations over land surfaces showed fairly large scatter, probably due to the large sensitivity of A and B to the stability and baroclinicity of the PBL (Sorbjan, 1989). More recently, Nicholls (1985) used the mean flow and turbulence data obtained over the ocean during the Joint Air–Sea Interaction Experiment (JASIN) to estimate $A \cong 1.4$ and $B \cong 4.2$. From Equations (10.19) and (10.20), the geostrophic drag coefficient can be expressed as

$$c_g = k[(\ln c_g + \ln Ro - A)^2 + B^2]^{-1/2} \quad (10.21)$$

where $Ro = G_0/fz_0$ is the surface Rossby number. Thus, c_g is a decreasing function of Ro ; its evaluation and plot is left as an exercise for the reader.

10.4 Turbulence

Turbulence in a neutrally stratified boundary layer is entirely of mechanical origin and depends on the surface friction and vertical distribution of wind shear. From similarity considerations discussed in Section 10.1, the primary velocity scale is u_* and normalized standard deviations of velocity fluctuations (σ_u/u_* , σ_v/u_* , and σ_w/u_*) must be constants in the surface layer and some functions of the normalized height fz/u_* in the outer layer. Surface layer observations from different sites indicate that under near-neutral conditions $\sigma_u/u_* \cong 2.4$, $\sigma_v/u_* \cong 1.9$, and $\sigma_w/u_* \cong 1.3$ (Panofsky and Dutton, 1984, Chapter 7). Observed values of turbulence intensity (σ_u/U) are shown in Figure 10.11 as a function of the roughness parameter. These are compared with the theoretical relation $\sigma_u/U = l/\ln(z/z_0)$, which is based on $\sigma_u/u_* = 2.5$ and the logarithmic wind-profile law. The above theoretical relation seems to overestimate turbulence intensities over very rough surfaces. Counihan (1975) has suggested an

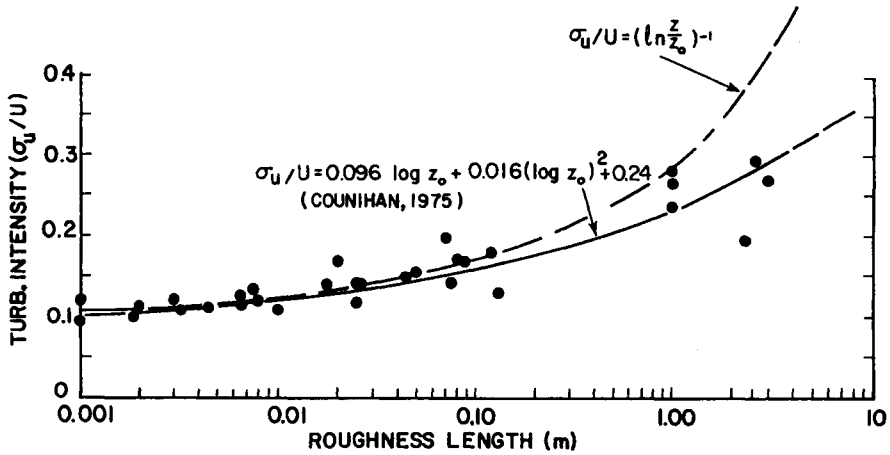


Figure 10.11 Variation of turbulence intensity in the near-neutral surface layer with the roughness length. [After Counihan (1975). Reprinted with permission from *Atmospheric Environment*. Copyright © (1975), Pergamon Journals Ltd.]

alternative empirical relationship between σ_u/U and $\log z_0$, which provides a better fit to the observed data in Figure 10.11.

Measurements of turbulence in the upper part of the near-neutral PBL are limited to few experiments in the marine PBL (Pennell and LeMone, 1974; Nicholls, 1985) but numerical model results indicate approximately exponential decrease of σ_u/u_* , etc., with height. For rough estimates of turbulent fluctuations, we suggest the following relations:

$$\begin{aligned}\sigma_u/u_* &= 2.4 \exp | - afz/u_* | \\ \sigma_v/u_* &= 1.9 \exp | - afz/u_* | \\ \sigma_w/u_* &= 1.3 \exp | - afz/u_* |\end{aligned}\quad (10.22)$$

in which the constant a may depend on the empirical constant c in the PBL height relationship $h = cu_*/|f|$. If we define the PBL height as the level where turbulent kinetic energy or momentum flux reduces to 10% of its value at the surface, then, we find that $a = 1.15/c$ (e.g., for $c = 0.25$, $a = 4.6$). Note that the above relations (10.22) imply the following expression for the TKE:

$$E = 5.5u_*^2 \exp | - 2afz/u_* | \quad (10.23)$$

Example Problem 2

For the wind profile data given in the Example Problem 1 for a site in southern Australia (latitude = 34.5°S), estimate the following turbulence parameters at the indicated heights in the neutral PBL:

- (a) the drag coefficient for $z_r = 10$ m;
- (b) the vertical turbulence intensities at 10 and 100 m;
- (c) turbulence kinetic energy (TKE) near the surface;
- (d) TKE at 100, 200, and 500 m.

Solution

- (a) We can estimate the wind speed at 10 m

$$U_{10} = \frac{u_*}{k} \ln \frac{z}{z_0} = \frac{0.485}{0.40} (\ln 10 + 7.15) = 11.46 \text{ m s}^{-1}$$

Then, $C_D = (u_*/U_{10})^2 = 1.79 \times 10^{-3}$.

- (b) In the surface layer,

$$\sigma_w = 1.3u_* = 0.63 \text{ m s}^{-1}$$

The vertical turbulence intensity is defined as

$$i_w = \sigma_w / U$$

and depends on the wind speed at a given height.

At $z = 10$ m,

$$i_w = \frac{\sigma_w}{U_{10}} = 0.055$$

Similarly, at $z = 100$ m,

$$i_w = \frac{\sigma_w}{U_{100}} = 0.044$$

- (c) Turbulence kinetic energy near the surface is given by

$$\begin{aligned} E &= \frac{1}{2}(\overline{u^2} + \overline{v^2} + \overline{w^2}) \\ &= \frac{1}{2}[(2.4)^2 + (1.9)^2 + (1.3)^2]u_*^2 \\ &\cong 5.5u_*^2 = 1.29 \text{ m}^2 \text{ s}^{-2} \end{aligned}$$

- (d) For estimating TKE at higher levels in the PBL, we use Equation (10.23) with $a = 4.6$. For the given latitude $\phi = -34.5^\circ$

$$f = 2\Omega \sin \phi = -0.826 \times 10^{-4} \text{ s}^{-1}$$

Then, the estimated values of TKE at various heights are:

z (m):	100	200	500
E ($\text{m}^2 \text{s}^{-2}$):	1.11	0.95	0.59

The estimated PBL height $h = 0.25u_* / |f| \cong 1468$ m.

10.5 Applications

Semiempirical wind-profile laws and other relations discussed in this chapter may have the following practical applications:

- Determining the wind energy potential of a site.
- Estimating wind loads on tall buildings and other structures.
- Calculating dispersion of pollutants in very windy conditions.
- Characterizing aerodynamic surface roughness.
- Parameterizing the surface drag in large-scale atmospheric models, as well as in wave height and storm surge formulations.

Problems and Exercises

1. Show that in the constant-stress surface layer, the power-law wind profile [Equation (10.2)] implies a power-law eddy viscosity profile [Equation (10.3)] and that the two exponents are related as $n = 1 - m$.
2. Derive the logarithmic wind-profile law on the basis of von Karman's mixing-length hypothesis, which implies

$$l_m = k \frac{\partial U}{\partial z} \bigg/ \frac{\partial^2 U}{\partial z^2}$$

in the constant-stress surface layer.

3. Using the logarithmic wind-profile law, plot the expected wind profiles (using a linear height scale) to a height of 100 m for the following combinations of the roughness parameter (z_0) and the mean wind speed at 100 m:

- (a) $z_0 = 0.01$ m; $U_{100} = 5, 10, 15$, and 20 m s^{-1} ;
- (b) $U_{100} = 10 \text{ m s}^{-1}$; $z_0 = 10^{-3}, 10^{-2}, 10^{-1}$, and 1 m.

Also calculate for each profile the friction velocity u_* and the drag coefficient C_D for a reference height of 10 m, and show their values on the graphs.

4. The following mean velocity profiles were measured during the Wangara Experiment conducted over a uniform short-grass surface under near-neutral stability conditions:

Height (m):	0.5	1	2	4	8	16
U (m s^{-1}):	4.91	5.44	6.06	6.64	7.17	7.71

- (a) Determine the roughness parameter and the surface stress for the above observation period. Take $\rho = 1.25 \text{ kg m}^{-3}$.
- (b) Estimate eddy viscosity, mixing length, and turbulence intensities at 5 and 50 m heights.

5. If the sea surface behaves like a smooth surface at low wind speeds ($U_{10} < 2.5 \text{ m s}^{-1}$), like a completely rough surface at high wind speeds ($U_{10} > 7.5 \text{ m s}^{-1}$), and like a transitionally rough surface at speeds in between, express and plot the drag coefficient C_D as a function of U_{10} in the range $0.5 \leq U_{10} \text{ m s}^{-1} \leq 50$, assuming the following:

- (a) $z_0 = 0.13 \nu/u_*$ in the aerodynamically smooth regime;
- (b) $z_0 = 0.02 u_*^2/g$ in the aerodynamically rough regime;
- (c) $z_0 = 2 \times 10^{-4} \text{ m}$ in the transitional regime.

6.

- (a) Derive the geostrophic drag relations (10.20) for the neutral PBL from the matching of the geostrophic departure laws (10.11) with the logarithmic wind profile law. Note that both the mean velocity and its vertical gradient should be matched in the surface layer.
- (b) Using Equation (10.21) with $A = 1.4$ and $B = 4.2$ for the neutral barotropic PBL, calculate and plot the geostrophic drag coefficient (c_g) as a function of the surface Rossby number (Ro) for the wide range of expected values of the latter (say, $Ro = 10^4$ – 10^9).

7.

- (a) Plot σ_u/u_* , σ_v/u_* , σ_w/u_* , and E/u_*^2 as functions of the normalized height fz/u_* in the neutral PBL, using $a = 4.6$.
- (b) After comparing the computed profiles of E/u_*^2 versus fz/u_* for $a = 3.5$ and 5.5 , discuss the sensitivity of the TKE profile to the empirical constant c in the PBL height relation $h = c|u_*/f|$. In order to remove the dependence on a or c , express E/u_*^2 as an exponential function of z/h .